Volume 14
Number 26
14 July 2023
Pages 3047-3138

Polymer Chemistry

rsc.li/polymers

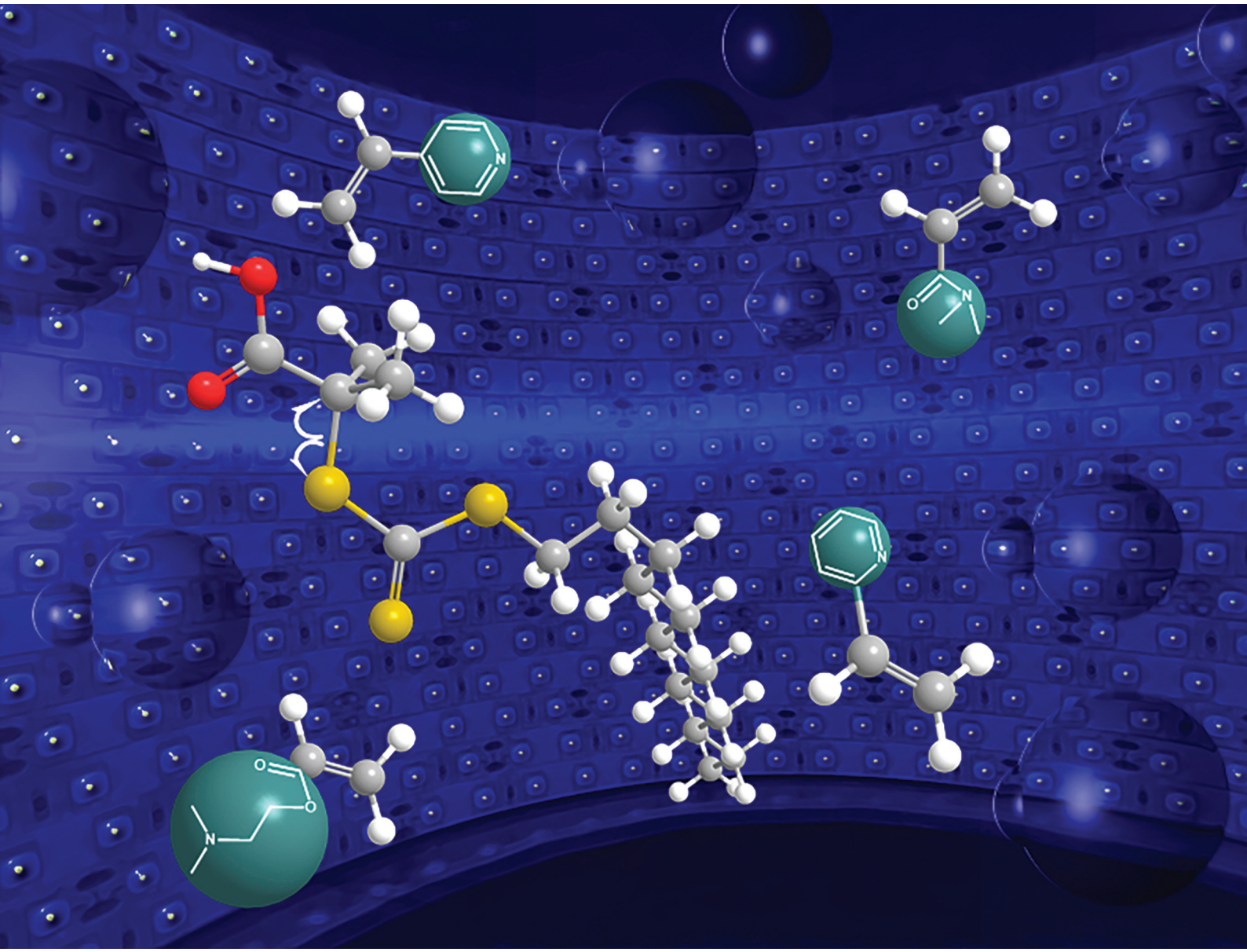

ISSN 1759-9962

PAPER

Maryam Radjabian, Volker Abetz *et al.*

Blue light-induced iniferter RAFT polymerization in aqueous-alcoholic media as a universal tool for the homopolymerization of various monomer families: kinetic investigations on different scales

ROYAL SOCIETY OF CHEMISTRY

Polymer Chemistry

ROYAL SOCIETY OF CHEMISTRY

PAPER

View Article Online
View Journal | View Issue

Cite this: *Polym. Chem.*, 2023, **14**, 3063

Blue light-induced iniferter RAFT polymerization in aqueous-alcoholic media as a universal tool for the homopolymerization of various monomer families: kinetic investigations on different scales†

Lara Hub, [a,b] Joachim Koll, [a] Maryam Radjabian *[a] and Volker Abetz *[a,b]

Photo-iniferter RAFT polymerization offers an opportunity to synthesize polymers without the requirements of external initiators. Blue light-induced iniferter RAFT polymerization was performed in a water–ethanol mixture (50 : 50 *w*/*w*) as an environmentally friendly, facile and tunable method to prepare well-defined homopolymers of different monomer classes like poly(*N*,*N*-dimethylacrylamide) (PDMA), poly(2-dimethylamino ethylacrylate) (PDMAEA) and poly(vinylpyridines) (PVPs). Homopolymers were synthesized on different laboratory scales between 1 g and 75 g. The influence of light intensity and temperature on polymerizations on different scales was investigated. Polymerization conditions were optimized and narrow molecular weight-distributed PDMA (*Đ* = 1.08–1.30), PDMAEA (*Đ* = 1.21–1.42), P4VP (*Đ* = 1.07–1.31) and P2VP (*Đ* = 1.14–1.35) were synthesized on larger laboratory scales and in short polymerization times (≤ 6 h). This study highlights the versatile usability and adaptability of visible light-induced RAFT polymerization for larger polymer production in a batch process.

Received 6th March 2023,
Accepted 8th May 2023

DOI: 10.1039/d3py00241a

rsc.li/polymers

Introduction

The development of reversible-deactivation radical polymerization (RDRP) techniques (previously called controlled radical polymerizations (CRPs))[1,2] like nitroxide-mediated polymerization (NMP),[3–5] atom transfer radical polymerization (ATRP)[6,7] and reversible addition–fragmentation chain transfer (RAFT) polymerization[8] has revolutionized the field of radical polymerization. Since these techniques closely imitate the characteristics of living polymerization,[9] they provide important improvements over the classical radical polymerization. Tailor-made polymers with predictable molecular weight, low dispersity (*Đ*), high end-group fidelity and capacity for continued chain growth can be obtained. RAFT controls the polymerization of a broad range of functional monomers and is compatible with a wide range of solvents and reaction conditions and is therefore, up to now, the most versatile RDRP technique.[10]

Within the last few decades, new methods were established to externally regulate the RAFT polymerization. Apart from traditional thermal initiation, alternative initiation methods *via* external stimuli have attracted wide interest.[11] More recently, photo-induced RAFT polymerization has gained considerable attraction. Most of the criteria for an ideal system are met by photo-initiation since light is a cheap, environmentally friendly, easily and widely accessible, non-invasive source and has no release of volatile organic compounds (VOCs).[11,12] Moreover, it provides spatiotemporal control and allows to adjust the radical concentration independent of the reaction temperature.[13] This ability to conduct photo-initiated polymerization under mild reaction conditions makes it so distinctive.[14] Nevertheless, especially for monomers with a small propagation rate constant (k_p) value, sufficient thermal energy must be provided for monomer propagation (according to Arrhenius equation) in order to carry out polymerization efficiently. The often-mentioned polymerization at room temperature is only suitable for fast propagating monomers, otherwise very long polymerization times are required and make the photopolymerization ineffective.

PhotoRAFT benefits from the versatility that the RAFT agent itself can be selectively photoactivated either *via* the usage of a photoredox catalyst such as a transition metal catalyst[15] or an organic dye molecule[16] (photo-induced electron/energy transfer (PET)-RAFT)[17,18] or *via* the photo-iniferter process. The iniferter (initiator transfer agent-terminator)[19,20] process is easy to handle since it does only require the chain transfer agent (CTA), monomer and solvent and not any exogenous radical

[a]*Helmholtz-Zentrum Hereon, Institute of Membrane Research, Max-Planck-Straße 1, 21502 Geesthacht, Germany. E-mail: maryam.radjabian@hereon.de*
[b]*Institute of Physical Chemistry, University of Hamburg, Martin-Luther-King-Platz 6, 20146 Hamburg, Germany. E-mail: volker.abetz@uni-hamburg.de*

† Electronic supplementary information (ESI) available. See DOI: https://doi.org/10.1039/d3py00241a

source or photocatalyst radical (see Scheme 1(a)). By usage of thiocarbonylthio CTAs, initiation occurs *via* direct photoactivation of the CTA, generating a persistent thiocarbonylthio radical which acts as controlling agent and a transient radical which initiates the polymerization[21] (see Scheme 1(b)), exemplary with 2-(dodecylthiocarbonothioylthio)-2-methylpropionic acid (DDMAT). For the light-initiation, an accurate selection of the light emitting source is important since the energy of the emitting photons is related to the wavelength and thus responsible for the electronic transition to higher energetic orbitals.[22] However, the light intensity influences the amount of photons and therefore the radical concentration and the propagation rate.[23] The absorption of the thiocarbonylthio (TCT) group of RAFT agent is mainly located in the UV region. Due to the high energy of UV light, unfortunately side reactions like the decomposition of RAFT agent were observed leading to loose living behaviour of the RAFT polymerization.[24,25] Therefore, to increase chain-end fidelity, the TCT group can be also activated by the second absorption band utilizing visible light sources.[26] The absorption band in the visible light region is much weaker and give the TCT RAFT agents the typical yellow colour (see Fig. S1†).[27] Herein, light-emitting diodes (LEDs) have been proven as efficient light sources for visible light-initiated RAFT polymerizations. They require low energy and operating costs and exhibit a longer lifetime compared to other light sources. On top, they emit nearly monochromatic light with less harmful UV rays and no IR radiation and therefore less heat is generated.[12,13,24] First reports on visible light-induced iniferter RAFT polymerization was conducted by the group of Boyer[28] and Qiao[26] in the mid 2010s for polymerization of methacrylate, diverse acrylates and *N*-isopropylacrylamide (NIPAM) utilizing a blue LED strip. Followed by blue light-induced iniferter polymerization of vinylactetate,[29] visible light-iniferter RAFT polymerization has shown to be an effective tool to synthesize diverse homopolymers. While several groups have already investigated the visible light-induced polymerization of (meth)acrylates and (meth)acrylamides, polymerization of vinylpyridines was rarely studied so far, especially the kinetics and optimization of the synthesis conditions of 2VP and 4VP *via* RAFT polymerization.[30] Nieswandt *et al.* synthesized diverse PVP homopolymers *via* traditional thermal RAFT polymerization in bulk.[31,32] With visible light initiation, so far only Xin and co-workers described the blue light iniferter RAFT polymerization of 2VP and utilized high 2VP weight fractions in the solution and low degree of polymerization.[27]

Besides blue light, photolysis of several RAFT agents can be as well initiated by green light and provides good control for the polymerization of methacrylates.[33] Recently, Xu and Abetz have shown that graft copolymers can be synthesized *via* the visible-light induced iniferter RAFT polymerization by selective excitation of different RAFT functionalities by green and blue light.[34,35] Therefore, due to its advantages, visible light-induced iniferter RAFT polymerization has gained increasing interest for the synthesis of well-defined polymers. However, it has been remarked as a disadvantage of photo-initiation that

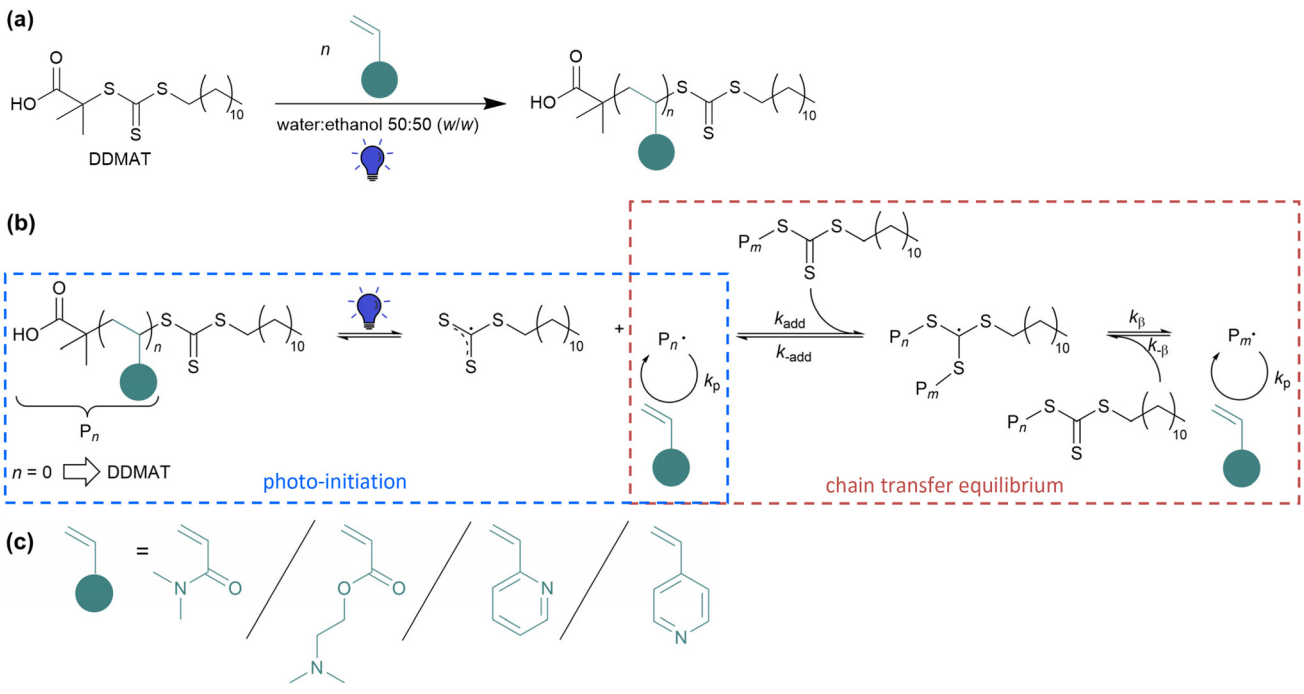

Scheme 1 (a) Synthetic route towards diverse macroCTAs *via* blue light-induced iniferter RAFT polymerization utilizing a home-made blue LED light source. (b) Mechanism of the blue light-induced RAFT polymerization with the RAFT agent DDMAT. Initiation occurs by the photo-induced cleavage of the C–S bond. The transient radical can propagate and take part in the chain transfer equilibrium. (c) Chemical structure of the monomers *N*,*N*-dimethylacrylamide (DMA), (2-dimethylamino ethylacrylate) (DMAEA), 2-vinylpyridine (2VP) and 4-vinylpyridine (4VP).

an increased reactor dimension hinders the polymerization procedure in a scale-up in a batch process.[36,37] Photo-induced polymerizations are significantly determined by other external factors such as light intensity and reactor dimensions and therefore it is important to study the influence of these parameters for the iniferter RAFT polymerization. Therefore, we investigate the influence of the batch reactor dimensions on a variety of homopolymerizations of fast and slowly propagating monomers.

Herein, we report an initiator- and catalyst-free blue light-induced iniferter RAFT polymerization of poly(*N*,*N*-dimethylacrylamide) (PDMA), poly(2-dimethylamino ethylacrylate) (PDMAEA), poly(2-vinylpyridine) (P2VP), and poly(4-vinylpyridine) (P4VP) homopolymers (see Scheme 1) in batches with dimensions between 10 mL and 500 mL reaction volume. A home-made blue LED is utilized to initiate the polymerization *via* direct activation of the TCT functionality. In order to make the polymerization procedure more sustainable, a water–ethanol mixture was used as solvent system, also for the rather nonpolar vinylpyridine monomers. This is an improvement towards the conventionally used petroleum-based solvents and demonstrates the versatility of the water-alcoholic mixture (50 : 50 *w*/*w*) for RAFT homopolymerizations. Synthesis conditions for each polymerization are kinetically investigated and optimized. The effect of dimensions of the glass vial towards the kinetics of the homopolymerization is studied showing the applicability of the batch process up to 500 mL reaction volume.

Experimental

Photoreactor setup

For the blue light-initiated RAFT polymerizations, a self-made cylindrical photoreactor was designed in which two LED strips (each with a length of 500.0 cm and 120 LEDs per m (Seki®)) were attached to the inner lower part of the aluminum cylinder (inner diameter: 18.0 cm, height: 25.0 cm, see Fig. S2†). The light intensity was adjusted by a MiLight® MiBoxer® RGB LED Controller regulated by a MiLight® remote control.

Materials

Ultrapure water (Milli-Q® quality, resistivity >18.2 MΩ cm^{-1}) was obtained from a Milli-Q® water purification system (Siemens Labostar). All other solvents including ethanol (≥99.9%, Merck), *N*,*N*-dimethylformamide (DMF) (≥99.8%, Merck), tetrahydrofuran (THF) (≥99.8%, Merck), cyclohexane (≥99.5%, Carl Roth) were used as received. Deuterium oxide (D_2O), deuterated methanol (MeOH-d_4) and chloroform ($CDCl_3$) were purchased from Deutero GmbH. As RAFT agent, 2-(dodecylthiocarbonothioylthio)-2-methylpropionic acid (DDMAT) (Sigma-Aldrich, stored at 4 °C) was used without further purification. 4-Vinylpyridine (4VP) (Thermo Scientific) was distilled prior polymerization to get deinhibited and colorless monomer. *N*,*N*-dimethylacrylamide (DMA) (Sigma Aldrich), 2-dimethylamino ethylacrylate (DMAEA) (Sigma-Aldrich) and 2-vinylpyridine (2VP) (Thermo Scientific) were deinhibited over activated basic aluminum oxide (Carl Roth) prior to each polymerization.

Synthesis of PDMA macroCTA *via* blue light-induced iniferter RAFT solution polymerization

In a typical photo-iniferter RAFT polymerization of DMA with a molar ratio of $[DMA]_0/[DDMAT]_0$ = 500/1, DDMAT (15.0 mg, 41.1 μmol, 1.0 eq.) and DMA (2.12 mL, 20.6 mmol, 500 eq.) were dissolved in ethanol (5.21 mL). While stirring, water (4.11 mL) was added dropwise and *N*,*N*-dimethylformamide (20 μL) added as an internal reference for ^{1}H-NMR analysis and an initial sample was taken. The solution was degassed by purging the ice-cooled polymerization vial with argon for 10 min. The polymerization vessel was placed at the centre of the blue LED. Polymerization was carried out under blue light irradiation (λ_{max} = 451 nm) at a water bath temperature of 40 °C under constant stirring (400 rpm). After the desired time of exposure to the blue light, the polymerization was stopped by turning off the irradiation source, quenching in an ice-cooling bath and exposing to air. The solvent was removed by vacuum and the crude polymer was obtained by drying under vacuum at 40 °C for 24 h. Subsequently, the polymer was dissolved in THF, precipitated in cold cyclohexane, filtered and dried under vacuum at 40 °C for 48 h.

The blue light-induced iniferter polymerization of the other monomers is followed by the same protocol and can be found in the ESI.†

General protocol of polymerizations in 250 mL and 500 mL vessels. The molar ratio between the substances and the general protocol were left unchanged apart from the longer argon-purging period of 30 min.

Characterization

NMR spectroscopy. ^{1}H-NMR spectra were recorded at ambient temperature using a Bruker® AV500 spectrometer with 16 scans per spectrum and a delay of 3 s. The samples from the homopolymerization of DMA were measured in D_2O and of DMAEA, 2VP and 4VP in MeOH-d_4. The determination of the monomer conversion and the theoretical molecular weight $\bar{M}_{n,th}$ is explained in the ESI.† Analysis was performed with the program MestReNova® 14.2.

Size exclusion chromatography (SEC). Size exclusion chromatography (SEC) experiments were conducted at 50 °C using dimethylacetamide (DMAc) as solvent with LiCl (0.1 M). Samples were measured at a flow rate of 1.0 mL min^{-1} using a Hitachi® L2130 pump. A PSS® GRAM pre-column (dimension 8 × 50 mm) and two PSS® GRAM columns (8 × 300 mm, particle size 10 μm) with a porosity of 3000 Å and 1000 Å, respectively, were used. The analysis was conducted with the signal recorded by a Hitachi® L2490 RI refractive index detector as a function of time. The instrumentation was calibrated with the use of polystyrene standards and the data were analyzed using the software PSS® Win GPC UniChrom V8.10.

Light intensity measurement. The light intensity of the blue LED was determined with an Ocean Insight® FLAME-T-UV-VIS spectrometer with QP400-2-SR-BX optical fiber and cosine cor-

rector. The sensor was placed at different positions within the cylinder and the height was varied in 2 cm steps. The light intensity was measured upwards and downwards and was afterwards summed to determine a more precise light intensity. The denoted light intensity is referred to the averaged light intensity at the different high positions.

UV-Vis Spectroscopy. UV-Vis-spectra were recorded using a Cary® 5000 UV-VIS-NIR or a Shimadzu® UVmini-1240 spectrophotometer. Ethanol served as solvent to dilute the RAFT agent.

Results and discussion

Herein, blue light-induced iniferter RAFT solution polymerization of DMA, DMAEA and vinylpyridines using DDMAT as RAFT agent are presented. DDMAT was used as an universal RAFT agent showing good control of the polymerization of more activated monomers (MAMs) like acrylates, acrylamides and aromatic vinyl monomers.[38–41] The DDMAT RAFT agent absorbs in the UV region (265 nm–365 nm) due to the spin allowed $\pi \rightarrow \pi^*$ electronic transition of the thiocarbonyl group and the absorption in the visible light region (385 nm–545 nm) is caused by the spin forbidden $n \rightarrow \pi^*$ electronic transition (see Fig. S1†). Photo-iniferter RAFT polymerizations were conducted by activating the thiocarbonyl adsorption band of DDMAT in the visible light region by blue light irradiation. For this purpose, a home-made photo reactor was installed. The aluminum basis provides high thermal conductivity to avoid possible overheating of the LEDs. A cylindrical geometry was chosen to achieve an optimal three-dimensional illumination of the polymerization solution. The design is particularly cost-effective, and the light intensity is homogeneous throughout the entire height irradiation area (see Fig. S3†). Additionally, the installed controller allows adjustment of light intensities by switching the voltage of the LED stripes (see Fig. 1(a), exemplary for a position in the center and at a height of 6 cm). The voltage can be tuned in different steps from 13.2 V–23.9 V. The specified light intensity values refer to the averaged values over a height range up to 15 cm. By varying the voltage of the blue LED, same peak emission profiles are observed. The home-made LED device emits light at λ_{max} = 451 nm and therefore very close to the absorption maximum of the RAFT agent in the visible light region (see Fig. 1(b)), preserving optimal efficient light initiation conditions. Since photoRAFT polymerizations were performed with different vessel sizes, the distribution of the light intensity within the blue LED was determined. Fig. 1(c) shows the light intensity distribution of the blue light at λ_{max} = 451 nm in the relevant area of the photoreactor; the distance of 9 cm constitutes the centre of the photoreactor. Depending on the distance to the LED stripes, height-averaged light intensities between 46 mW cm^{-2} and 55 mW cm^{-2} are preserved by applying a voltage of 19.7 V at the blue LED. The light intensity given in the further course refers to the intensity at the edge of the surface of the vessel. For the polymerizations, an environmentally friendly ethanol-water mixed solvent was used. Ethanol serves as a cosolvent, is safe and categorized as a recommended solvent in terms of solvent selection.[42,43] Due to the good solubility of DDMAT, monomers (DMA, DMAEA and the vinylpyridine isomers), as well as resulting homopolymers, all the polymerizations were conducted in a solvent mixture of water–ethanol

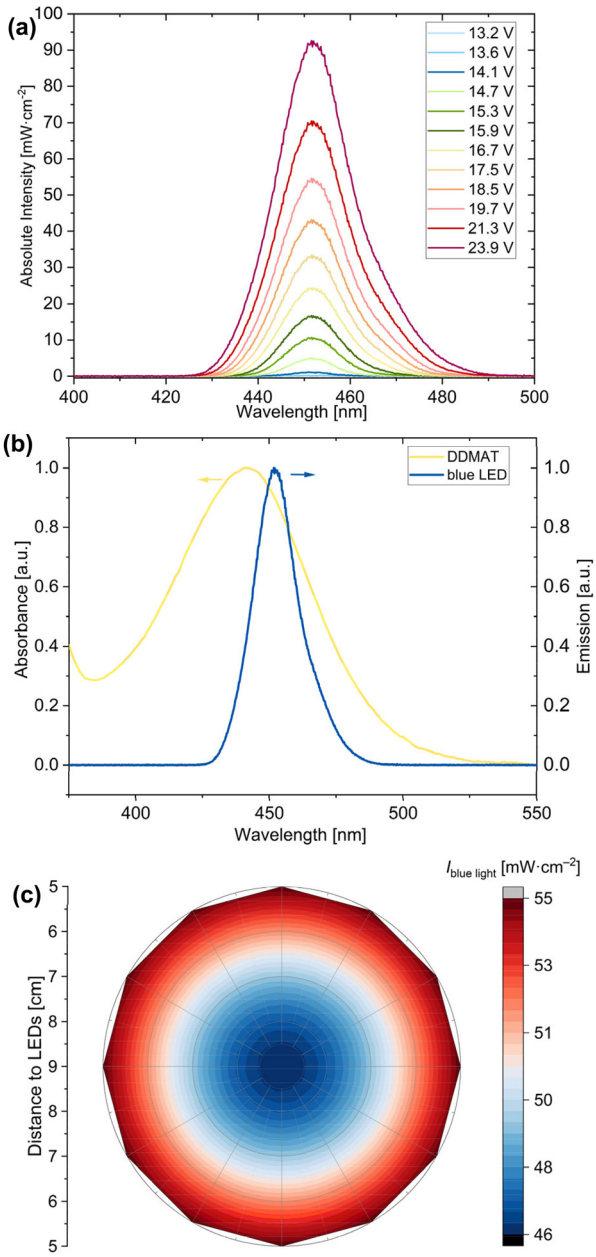

Fig. 1 (a) Light intensity spectrum of the blue LED at a height of 6 cm in dependence of the applied voltage. The maximum emission wavelength is at λ_{max} = 451 nm. (b) Comparison of the absorption of the RAFT agent DDMAT (in ethanol) in the visible light range due to the spin forbidden $n \rightarrow \pi^*$ electronic transition of the thiocarbonyl functionality and the emission spectrum of the blue LED. (c) Light intensity distribution of blue light at λ_{max} = 451 nm within the blue LED at an applied voltage of 19.7 V. For this purpose, the light intensities were measured up to the height of 15 cm and averaged in each radial position. The centre of the photoreactor is at a distance of 9 cm towards the LED stripes.

(50 : 50, *w*/*w*). In the following, sample codes are used (*e.g.*, PDMA^{z}), in which superscripts signify the overall theoretical number average molecular weight (in kDa).

Synthesis of PDMA *via* blue-light induced iniferter RAFT solution polymerization

Most literature reports the synthesis of PDMA by thermally initiated RAFT polymerization in petroleum based solvents like dioxane,[44–48] DMAc[49] or DMF[50,51] at temperatures ranging from 60 °C–80 °C. The polymerizations of DMA can be conducted in pure water with a water-soluble RAFT agent, however DDMAT is not soluble in water and thus ethanol as a cosolvent is required. Preliminary solubility tests of the RAFT agent in water–ethanol mixtures showed a good solubility of DDMAT in the (50 : 50 *w*/*w*) mixture. In the systems with higher water content the RAFT agent precipitates.

Herein, the light intensities have been varied to establish the blue light initiated RAFT solution polymerization in the water–ethanol mixture (50 : 50, *w*/*w*) towards well-defined PDMA macroCTAs without any further catalysts or initiators. The rate of cleavage of sulphur-carbon bonds is light intensity dependent. Therefore, it is expected that the radical concentration increases by applying a higher light intensity of the blue LED. Fig. 2(a) shows the illumination time-dependent conversion of DMA with $[DMA]_0/[DDMAT]_0$ = 500 by varying the light intensity of the blue LED. As expected, the conversion increases by increasing the light intensity. Interestingly, the polymerization conducted at 16 mW cm^{-2} shows a short inhibition time (<30 min) and afterwards, the conversion follows a linear slope by time. Under these conditions, the light intensity is the polymerization-rate determining factor. By increasing the light intensity further to 30 mW cm^{-2} and 49 mW cm^{-2}, high conversions within short polymerization times are reached and no inhibition period is observed. Within the first 2 h – probably even longer – these polymerizations follow pseudo-first-order kinetics (see Fig. 2(b)), indicating a constant concentration of propagating radical species during the polymerization. Noticeably, a sharp increase in conversion is recognized when the light intensity is increased from 16 mW cm^{-2} to 30 mW cm^{-2}. A further increase to 49 mW cm^{-2} slightly influences the conversion. Therefore, it is confirmed that by increasing light intensity of the blue LED a faster reaction is observed. This can be explained by the higher radical concentration obtained by increased light intensity. Apparent propagation rate constants $k_{p,app}$ are determined from the slope of the first order plot in Fig. 2(b) and are calculated to be 0.19 h^{-1}, 0.55 h^{-1} and 0.70 h^{-1}, respectively, and are therefore directly proportional to the light intensity (see Fig. 2(c)). However, in the photo-iniferter RAFT, the light intensity dependence of the apparent rate coefficient differs from that observed in the PET RAFT polymerization with the photocatalyst Ir(ppy)$_3$ due to the square root dependence of the apparent rate coefficient for the photocatalyst excitation process k_{EX}.[52]

A linear increase of apparent molecular weight $\bar{M}_{n,app}$ with conversion is observed (see Fig. 2(d)). The discrepancy of different evolution of $\bar{M}_{n,app}$ and $\bar{M}_{n,th}$ is caused by the different hydrodynamic radii of PDMA and PS standards in DMAc. Dispersities remain low over the complete polymerization (≤1.25) and show to be unaffected by the monomer conversion. Furthermore, no influence of light intensity on the dispersity of the PDMA homopolymers can be detected (see Table S1†).

In order to proof the temporal control over the polymerization of DMA, the blue light was periodically switched on and off in 30 min intervals (see Fig. 2(e)). When the light was switched on, polymerization occurred. By switching off the blue light, conversion was almost stopped; however, the preformed radicals can slightly react with the present monomers. This experiment confirms that the polymerization occurs only under visible light irradiation and shows the temporal control within this process.

With the aim to perform polymerization on different laboratory scales, 4 different vessels were used to perform the polymerization. In addition to the aforementioned polymerization scale of 20 mL, vessels with 40 mL, 250 mL and 500 mL volume were used. Synthesis of PDMA macroRAFT agent in larger vessels were performed under the same aforementioned conditions ($[DMA]_0/[DDMAT]_0$ = 500, 40 °C, voltage blue LED = 19.7 V). The 20 mL and 40 mL vessels have the same diameter of 2.5 cm. The 250 mL vessel possess a diameter of 6.0 cm and vessel with a volume of 500 mL has a diameter of 7.5 cm. Due to these different dimensions, the kinetics of this polymerization process change. The enlargement of the scale changes the distance to the LED strips and, as shown in Fig. 1(c), the light intensity is slightly altered. Adjusted by a voltage of 19.7 V, light intensity at the surface of each vessel is changed from 49 mW cm^{-2} (20 mL and 40 mL vials) to 52 mW cm^{-2} (250 mL vessel) to 55 mW cm^{-2} (500 mL vessel). Despite the slight increase in light intensity due to the increasing radius of the vessel, the final conversion of the polymerization in the 250 mL vessel decreased by 6% and in the 500 mL vessel decreased by 12% compared to the polymerization in 20 mL vessel (see Fig. 3(a)). However, polymerizations conducted in the vessels with 20 mL and 40 mL volume showed similar conversions. The penetrated light and therefore the radical concentration is determined by the exposed shell surface area $2\pi rh$ of a cylindrical vessel with r as the radius and h as the height. Since a similar intensity distribution in the photoreactor regardless of the height is dictated (see Fig. S3†), a similar number of photons per area penetrate the solution in all areas of the glass surface. According to our observations, the light intensity and thus the generation of radicals is significantly related to the radius of the vessels. Attributed to Beer–Lambert law $A = \log(I_0/I) = \varepsilon cl$ in which A is the absorbance, I_0 is the incoming and I the transmitted intensity, ε the molar extinction coefficient, c the molar concentration and l is the path length, in our case the absorption depends proportionally on the path length (all other factors remain constant). Since we have a three-dimensional symmetrical set-up, the path length corresponds to the radius of the vessel. Due to this, the polymerizations in the 20 mL and 40 mL vessels show the same kinetics. A similar observation was made for the PET

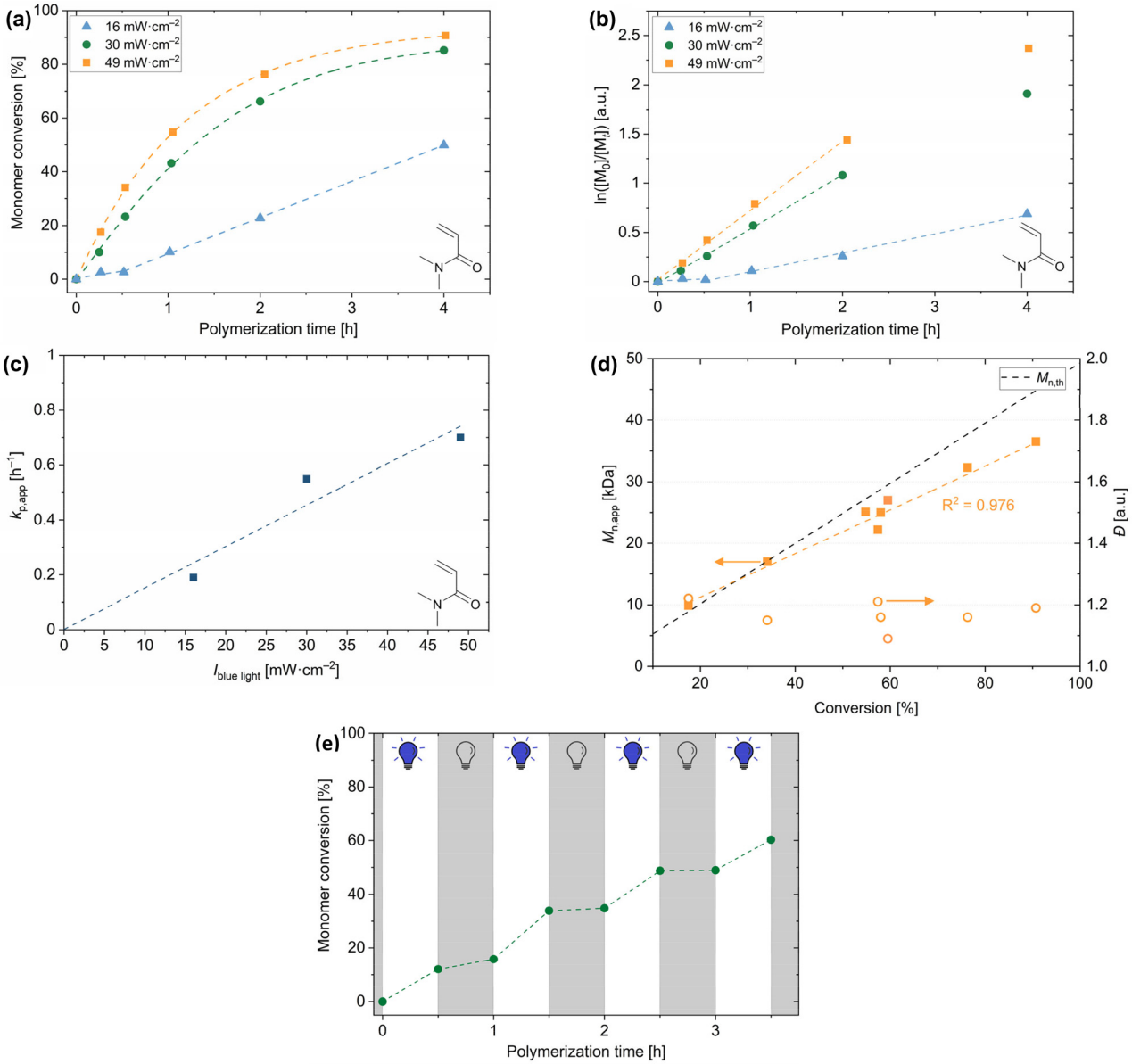

Fig. 2 (a) Monomer conversion and (b) pseudo first-order kinetic plots of blue light-initiated RAFT solution polymerization of DMA ($[DMA]_0/[DDMAT]_0$ = 500) in the water–ethanol mixture (50 : 50 *w*/*w*) (20% *w*/*w*) at 40 °C with different light intensities (referred to λ_{max} = 451 nm). (c) Linear dependence of the apparent propagation constant $k_{p,app}$ of the light intensity. (d) Evolution of $\bar{M}_{n,app}$ (solid squares) and dispersity (hollow points) with conversion of the blue-light initiated homopolymerization of DMA synthesized in the 20 mL vessels at 49 mW cm^{-2} ($M_{n,app}$ and $Đ$ were determined by analysis of SEC curves, eluent: DMAc, poly(styrene) calibration). (e) "On–off" kinetic plot of the blue light-induced DMA hompolymerization at 30 mW cm^{-2}.

RAFT polymerization of methyl acrylate with PADTC RAFT agent and the photocatalyst Ir(ppy)3.[52] By changing the reaction volume but keeping the diameter constant, similar reaction rates were observed. Calculations of the apparent propagation constants show that this constant decreases linearly with increasing vessel radius from 0.70 h^{-1} (20 mL vessel) to 0.57 h^{-1} (250 mL vessel) to 0.49 h^{-1} (500 mL vessel) as shown in Fig. 3(b), regardless of the slight change in light intensity on the surface. Despite the reduction of the conversion by vessel radius, the homopolymerization of DMA in all reaction volumes proceeds in a fast manner without any inhibition period. Even in the 500 mL vessels, polymers with low dispersity are obtained (see Fig. 3(c)). This shows the adaptability of the blue light-induced iniferter RAFT polymerization even for a larger production of PDMA homopolymers on the laboratory scale up to a yield of about 75 g polymer.

Synthesis of PDMAEA *via* blue-light induced iniferter RAFT solution polymerization

In order to investigate the efficiency of this synthesis procedure to acrylates, thermo and pH dual-responsive poly(2-(dimethylamino) ethyl acrylate) (PDMAEA) was synthesized. The

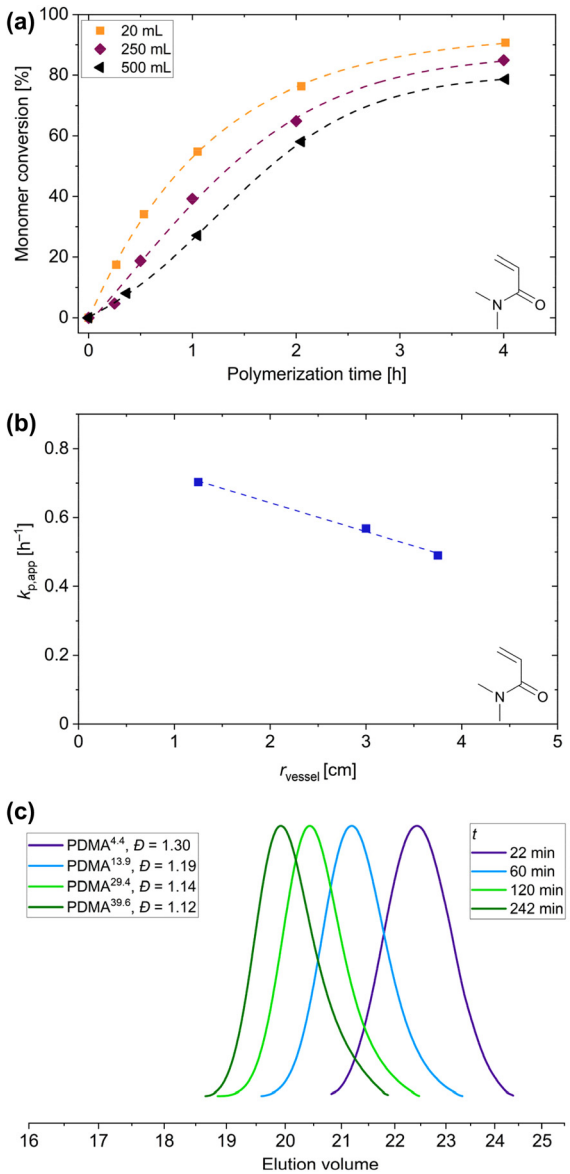

Fig. 3 (a) DMA conversion *via* blue light initiation at 19.7 V in dependence of the vessel size. (b) Dependence of the apparent propagation constant $k_{p,app}$ of the vessel radius. (c) SEC traces of the polymerization of DMA on 500 mL scale at a light intensity of 55 mW cm^{-2}.

polymerization conditions were adapted from the optimized conditions for DMA. Fig. 4(a) displays the conversion of the blue light-induced polymerization of DMAEA with $[DMAEA]_0/[DDMAT]_0$ = 500 in water–ethanol mixtures (50 : 50, *w*/*w*) at 40 °C and an adapted voltage of 19.7 V at the blue LED. Conversion in the small 20 mL vials decreased by almost 30% compared to DMA; the difference in conversion on a larger scale decreased by the same order of magnitude. Apparent propagation rate constants $k_{p,app}$ are determined to be 0.34 h^{-1} for the DMAEA polymerization in the 20 mL vessel and 0.26 h^{-1} for the polymerization in the 250 mL vessel. It indicates that DMAEA is slower in propagation than DMA in this photo-iniferter RAFT process. The same observation was made in the PET-RAFT polymerization by green light irradiation of these two monomers.[53] As observed for the polymerization of DMA, light-induced polymerization of DMAEA also proceeds in a first order fashion up to 2 h polymerization time (see Fig. 4(b)).

Synthesis of PVP *via* blue light-induced iniferter RAFT solution polymerization

Compared to the pre-discussed DMA and DMAEA, the vinylpyridine isomers are more slowly propagating in a RAFT process due to the mesomeric stabilization of the formed radicals. Therefore, the synthesis becomes more challenging. Herein, 4-vinylpyridine and 2-vinylpyridine were polymerized in the water–ethanol mixture (50 : 50, *w*/*w*) *via* blue light-induced iniferter solution polymerization. To the best of our knowledge, this is the first time to synthesize such VP polymers *via* RAFT in aqueous media under neutral pH conditions.

In order to study the influence of several reaction parameters on the kinetics, photo-iniferter RAFT polymerization of 4VP was systematically investigated with $[4VP]_0/[DDMAT]_0$ = 470. Fig. 5(a) shows the illumination time-dependent conversion of 4VP conducted with different monomer contents at a polymerization temperature of 40 °C. Whereas for the DMA and DMAEA polymerizations no induction period was observed under these synthesis conditions, an inhibition period is observed for the synthesis of 4VP in the small 40 mL polymerization vessel (<30 min) as well as in the 250 mL vessel (<1 h). The pre-equilibrium time frame is extended for the 4-vinylpyridine polymerization probably due to the smaller addition rate coefficient of the monomer to the RAFT agent (see Scheme 1(b)).[54] This leads to a longer reinitiation time and a slow transition from the pre- to the main equilibrium of the RAFT process and a retardation of the polymerization.

Compared to the above-mentioned monomers, the conversion of 4VP is significantly reduced. At comparable conditions in the small vessels with 20% (*w*/*w*) and 4 h polymerization time at 49 mW cm^{-2}, a conversion of 41% was reached, which is 50% less than for DMA and 21% less than for DMAEA. Apparent propagation constants $k_{p,app}$ are determined to be 0.15 h^{-1} for the polymerization in the vessel with 40 mL volume and 0.08 h^{-1} for the polymerization in the 250 mL vessel. Thus, compared to DMA, these values are lower by a factor of 4.7 for the small vessels and by a factor of 7.1 for the reaction in 250 mL vessel. Consequently, synthesis conditions were changed to generate a more effective polymerization. The influence of different key parameters such as temperature, light intensity and monomer concentration were systematically investigated. Due to the photo-iniferter mechanism, the initiation step is independent of temperature. Thus, increasing the reaction temperature assists the monomer addition but might lead to a higher termination rate. Moderately increasing the water bath temperature from 40 °C to 50 °C leads to an increase in conversion of more than 10% after 4 h polymerization time (see Table S8†). It indicates that for the monomer addition of 4-vinylpyridine a higher activation energy barrier must be overcome compared to DMA, although both mono-

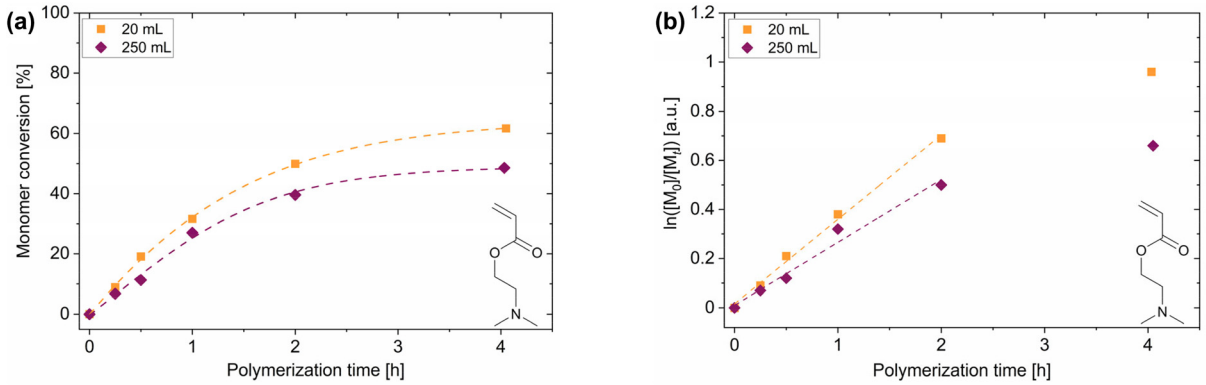

Fig. 4 (a) DMAEA conversion and (b) pseudo first-order kinetic plots of blue light-initiated iniferter RAFT solution polymerization of DMAEA ($[DMAEA]_0/[DDMAT]_0$ = 500) in water–ethanol mixtures (50 : 50 *w*/*w*) (20% *w*/*w*) at 40 °C and an adapted voltage of 19.7 V at the blue LED.

mers are considered as more activated monomers (MAMs).[9] A higher intensity leads to more frequent fragmentation and therefore to a higher radical concentration. By increasing the light intensity from 52 mW cm^{-2} to 86 mW cm^{-2}, conversion was enhanced by only 5% after 4 h polymerization time (see Table S12†). This shows that the increase in light intensity has little effect on conversion and radical generation is already very effective at 52 mW cm^{-2}. In order to investigate the influence of monomer concentration on conversion, concentration was increased to 30 (*w*/*w*) ($[4VP]_0/[DDMAT]_0$ = 470, see Fig. 5(a)). Conversion could be enhanced by 7% after a polymerization time of 4 h compared to the one with 20 (*w*/*w*). The solution viscosity was still low enough to guarantee a uniform mixture during the whole polymerization process. No influence of the monomer concentration on the dispersity of the P4VP macroCTAs was observed, neither for the polymers synthesized in the small vessels, nor in the 250 mL vessels (see Tables S8, 9, S11 and 12†). Therefore, executing the polymerization at 30% (*w*/*w*) is more attractive compared to 20% (*w*/*w*). The polymerization conditions can be adjusted to mitigate the decrease in 4VP conversion.

It has been shown that degradation of the thiocarbonyl functionality by time leads to the formation of dead polymer chains.[27] Therefore, in order to ensure high livingness of the P4VP homopolymers, the polymerization was stopped after 6 h. During this time, pseudo first-order kinetic plots show linear slope (see Fig. 5(b)).

By changing a reaction vessel from 40 mL to 250 mL and adapting the same voltage of 19.7 V, conversion decreased more distinctly compared to the previously mentioned monomers (around 25% after 6 h polymerization time at 30% (*w*/*w*), see Fig. 5(a)). The apparent propagation rate constant $k_{p,app}$ is reduced from 0.190 h^{-1} to 0.109 h^{-1} by choosing the larger scale. For 4VP as a monomer with a small propagation constant, conversion is strongly effected by scale enlargement. By choosing a light intensity of 86 mW cm^{-2} instead of 52 mW cm^{-2}, conversion increases by 6% after 6 h (see Table S12†). Another way to compensate the conversion decrease is to choose a higher temperature (see Table S12†).

In order to demonstrate the applicability of the light-induced iniferter polymerization to synthesize higher molecular weight polymers, 4VP was synthesized with a molar ratio of $[4VP]_0/[DDMAT]_0$ = 760 at 40 °C in a 250 mL vessel (see Table S13†). A $P4VP^{42.2}$ was synthesized with a low dispersity of 1.22. It indicates that the synthesis method is also suitable for higher $[4VP]_0/[DDMAT]_0$ ratios and the polymerization is still well controlled, although the DDMAT concentration is significantly decreased.

The effect of temperature on the kinetics of the blue light-induced polymerization of 2VP is even more significant than for 4VP and therefore studied here in detail. Fig. 5(c) illustrates the systematical investigation of the influence of temperature on the conversion of reaction in the small vessel (40 mL) in the temperature range between 40 °C and 70 °C. The position of the pyridinyl nitrogen atom in 2VP and 4VP dramatically influences the propagation rate in RAFT polymerization and therefore the course of the polymerization. When comparing the two polymerizations of 4VP and 2VP at 40 °C and 30% (*w*/*w*), an inhibition time prolonged by about 15 min is observed for the photoRAFT polymerization of 2VP. This is probably due to the smaller addition rate constant of 2VP compared to 4VP to the RAFT agent DDMAT. As well, only 35% 2VP conversion was reached after a polymerization of 6 h, whereas under similar reaction conditions a 4VP conversion of 65% was determined. This proves that even more thermal energy is required to promote the light-induced RAFT of polymerization of 2VP compared to 4VP for achieving comparable conversions. By increasing the reaction temperature from 40 °C to 70 °C, the conversion can increase by 23% to 58% after 6 h exposure to the blue light. Due to the temperature increase, apparent propagation rate constants $k_{p,app}$ enhance from 0.085 h^{-1} to 0.155 h^{-1}. Thus, the synthesis can be carried out efficiently at low polymerization time. This increase in the propagation constant can be explained by the fact that propagation is driven by thermal energy. At higher temperature, more thermal energy is available and thus more reactive species are above the activation energy level for the monomer addition. Thus, more collisions of the radical of the growing chain with monomer units

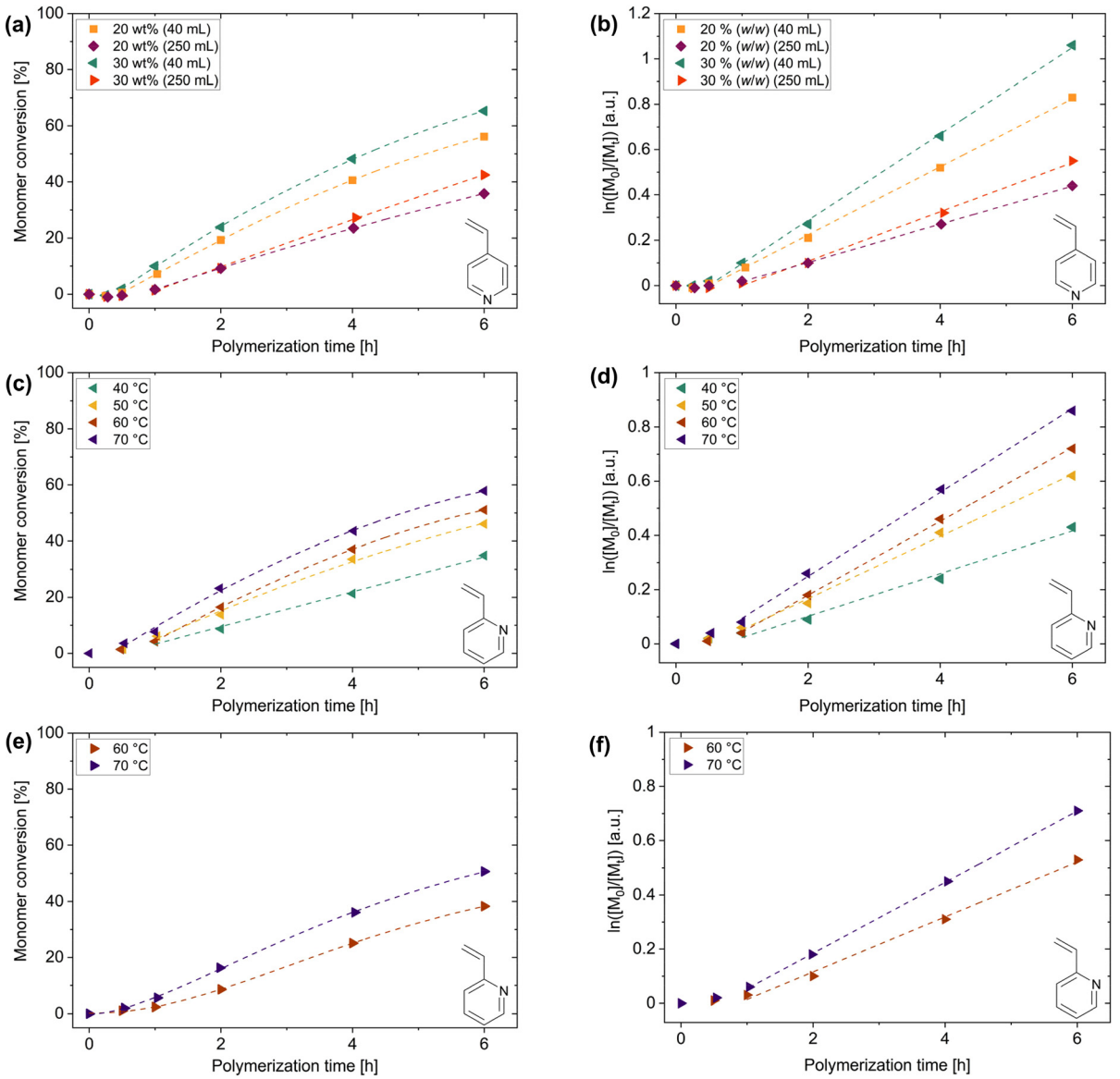

Fig. 5 (a) Monomer conversion and (b) pseudo first-order kinetic plots of blue light-initiated iniferter RAFT solution polymerization of 4VP ($[4VP]_0/[DDMAT]_0$ = 470, 40 °C, 19.7 V). (c) Monomer conversion and (d) pseudo first-order kinetic plots of blue light-initiated RAFT solution polymerization of 2VP on 40 mL scale at temperatures of 40 °C – 70 °C ($[2VP]_0/[DDMAT]_0$ = 470, 19.7 V). (e) Monomer conversion and (f) pseudo first-order kinetic plots of blue light-initiated RAFT solution polymerization of 2VP on 250 mL scale at temperatures of 60 °C and 70 °C ($[2VP]_0/[DDMAT]_0$ = 470, 19.7 V).

lead to chain extension. Pseudo first-order kinetic plots show linear behavior from 2 h (40 °C) or 1 h (50 °C–70 °C) (see Fig. 5(d)), indicating a constant radical concentration. Dispersites of P2VP macroCTAs remain low independent of polymerization temperature ($Đ$ = 1.09–1.36, see Table S14†).

From an energy point of view, a temperature increase towards 70 °C is reasonable, as this can significantly shorten the polymerization time. This is particularly important for larger scale applications since previous experiments showed that longer polymerization times are required in order to receive comparable conversions. As already observed for the photo-iniferter RAFT polymerization of 2VP in the small vessels, a temperature of 40 °C compared to 70 °C is associated with a doubling of the reaction time to reach same conversion. A rough estimation of the energy consumption for both synthesis in the 250 mL vessels in order to reach 50% conversion (see chapter 9†) shows an energy consumption of approx. 1.42 MJ for the synthesis at 40 °C and 12 h polymerization time and of 1.05 MJ for the synthesis conducted at 70 °C but only 6 h polymerization time. Therefore, adapting the polymerization conditions to shorter polymerization time and higher temperature leads to a bisection of the polymerization time and decreased energy consumption saving energy and manpower. Due to these findings, P2VP polymerizations in the

250 mL vessels were carried out only at 60 °C and 70 °C. Both polymerizations show a short inhibition period (<1 h) (see Fig. 5(e) and (f)) as observed likewise for the polymerisation in the small vials. After 6 h polymerization time, 2VP conversions of 41% and 51% were determined at polymerization temperatures of 60 °C and 70 °C, respectively, thus reduced by 10% and 7% by using a 250 mL vessel instead of the small ones. Polymers with low dispersities were obtained ($Đ$ = 1.14–1.35, see Table S15†). Therefore, especially the optimized synthesis at a temperature of 70 °C turns out to be robust approach for conducting the polymerization on a larger scale and presents a suitable synthesis procedure for larger production of tailor made P2VP homopolymer.

Conclusions

We developed and optimized routes to synthesize well-defined macroCTAs on different laboratory scales *via* RAFT polymerization induced by blue light without the use of exogenous initiators or catalysts. The switchable and uniform illumination *via* the cylindrical blue LED irradiation offers the possibility to adjust the radical generation and thus to influence the polymerization process. In combination with DDMAT as a suitable RAFT agent to control the polymerization in water–ethanol (50 : 50, *w*/*w*) solvent system, a versatile and environmentally friendly RAFT polymerization strategy for various monomer families is established. MAM classes encompassing acrylamides, acrylates and even rather nonpolar vinylpyridines (4- and 2-isomer) could be polymerized with good control despite the different apparent propagation constants. Due to the decoupling of the initiation from the thermal conditions, high DMA and DMAEA conversions can be achieved at a low ambient temperature of 40 °C after short polymerization times (≤ 4 h). Furthermore, we have shown that synthesis up to 500 mL scale is possible without significant loss of conversion. Comparably, 4VP as a slower propagating monomer in the RAFT process demonstrated a good control even at 40 °C polymerization temperature. While for DMA and DMAEA the same synthesis conditions can be used for the larger 250 ml scale, it is recommended to adjust the parameters for 4VP polymerization towards higher light intensities and/or temperatures. Visible light-induced polymerization of 2VP showed a strong temperature-dependence of the kinetics. We conclude that it is possible to reach relatively high conversions at 70 °C and a high robustness in terms of scalability. This adaptability of the synthesis conditions to the various monomers, even for the larger scales, is the strength of this polymerization approach.

Author contributions

Lara Hub: conceptualization, data curation, formal analysis, investigation, methodology, validation, visualization, writing – original draft, writing – review & editing; Joachim Koll: investigation, writing – review & editing; Maryam Radjabian: conceptualization, project administration, supervision, writing – review & editing; Volker Abetz: funding acquisition, resources, supervision, writing – review & editing.

Conflicts of interest

There are no conflicts to declare.

Acknowledgements

The authors thank Silvio Neumann, Petra Merten and Maren Brinkmann for NMR spectroscopy and SEC measurements. Further thanks go to Eugen Ebel for installing the blue LED and Dr. Thomas Emmler for the support of the light intensity measurements.

References

1 A. D. Jenkins, R. G. Jones and G. Moad, Terminology for reversible-deactivation radical polymerization previously called “controlled” radical or “living” radical polymerization (IUPAC Recommendations 2010), *Pure Appl. Chem.*, 2009, **82**, 483–491.
2 D. A. Shipp, Reversible-Deactivation Radical Polymerizations, *Polym. Rev.*, 2011, **51**, 99–103.
3 E. Rizzardo and D. H. Solomon, A new method for investigating the mechanism of initiation of radical polymerization, *Polym. Bull.*, 1979, **1**, 529–534.
4 G. Moad, E. Rizzardo and D. H. Solomon, Selectivity of the reaction of free radicals with styrene, *Macromolecules*, 1982, **15**, 909–914.
5 P. G. Griffiths, E. Rizzardo and D. H. Solomon, Quantitative studies on free radical reactions with the scavenger 1,1,3,3-tetramethylisoindolinyl-2-oxy, *Tetrahedron Lett.*, 1982, **23**, 1309–1312.
6 J.-S. Wang and K. Matyjaszewski, “Living”/Controlled Radical Polymerization. Transition-Metal-Catalyzed Atom Transfer Radical Polymerization in the Presence of a Conventional Radical Initiator, *Macromolecules*, 1995, **28**, 7572–7573.
7 M. Kato, M. Kamigaito, M. Sawamoto and T. Higashimura, Polymerization of Methyl Methacrylate with the Carbon Tetrachloride/Dichlorotris- (triphenylphosphine)ruthenium (II)/Methylaluminum Bis(2,6-di-tert-butylphenoxide) Initiating System: Possibility of Living Radical Polymerization, *Macromolecules*, 1995, **28**, 1721–1723.
8 J. Chiefari, Y. K. Chong, F. Ercole, J. Krstina, J. Jeffery, T. P. T. Le, R. T. A. Mayadunne, G. F. Meijs, C. L. Moad, G. Moad, E. Rizzardo and S. H. Thang, Living Free-Radical Polymerization by Reversible Addition–Fragmentation Chain Transfer: The RAFT Process, *Macromolecules*, 1998, **31**, 5559–5562.

9 S. Perrier, 50th Anniversary Perspective : RAFT Polymerization—A User Guide, *Macromolecules*, 2017, **50**, 7433–7447.
10 D. J. Keddie, A guide to the synthesis of block copolymers using reversible-addition fragmentation chain transfer (RAFT) polymerization, *Chem. Soc. Rev.*, 2014, **43**, 496–505.
11 F. A. Leibfarth, K. M. Mattson, B. P. Fors, H. A. Collins and C. J. Hawker, External regulation of controlled polymerizations, *Angew. Chem., Int. Ed.)*, 2013, **52**, 199–210.
12 C. Dietlin, S. Schweizer, P. Xiao, J. Zhang, F. Morlet-Savary, B. Graff, J.-P. Fouassier and J. Lalevée, Photopolymerization upon LEDs: new photo-initiating systems and strategies, *Polym. Chem.*, 2015, **6**, 3895–3912.
13 M. Chen, M. Zhong and J. A. Johnson, Light-Controlled Radical Polymerization: Mechanisms, Methods, and Applications, *Chem. Rev.*, 2016, **116**, 10167–10211.
14 X. Pan, M. A. Tasdelen, J. Laun, T. Junkers, Y. Yagci and K. Matyjaszewski, Photomediated controlled radical polymerization, *Prog. Polym. Sci.*, 2016, **62**, 73–125.
15 S. Shanmugam, J. Xu and C. Boyer, Photo-induced Electron Transfer–Reversible Addition–Fragmentation Chain Transfer (PET-RAFT) Polymerization of Vinyl Acetate and N -Vinylpyrrolidinone: Kinetic and Oxygen Tolerance Study, *Macromolecules*, 2014, **47**, 4930–4942.
16 J. C. Theriot, G. M. Miyake and C. A. Boyer, N,N-Diaryl Dihydrophenazines as Photoredox Catalysts for PET-RAFT and Sequential PET-RAFT/O-ATRP, *ACS Macro Lett.*, 2018, **7**, 662–666.
17 J. Xu, K. Jung, A. Atme, S. Shanmugam and C. Boyer, A robust and versatile photo-induced living polymerization of conjugated and unconjugated monomers and its oxygen tolerance, *J. Am. Chem. Soc.*, 2014, **136**, 5508–5519.
18 M. L. Allegrezza and D. Konkolewicz, PET-RAFT Polymerization: Mechanistic Perspectives for Future Materials, *ACS Macro Lett.*, 2021, **10**, 433–446.
19 T. Otsu and M. Yoshida, Efficient synthesis of two or multi component block copolymers through living radical polymerization with polymeric photo-iniferters, *Polym. Bull.*, 1982, **7**, 197–203.
20 T. Otsu and M. Yoshida, Role of Initiator-Transfer Agent-Terminator (Iniferter) in Radical Polymerizations: Polymer Design by Organic Disulfides as Iniferters, *Makromol. Chem., Rapid Commun.*, 1982, **3**, 127–132.
21 M. Semsarilar and V. Abetz, Polymerizations by RAFT: Developments of the Technique and Its Application in the Synthesis of Tailored (Co)polymers, *Macromol. Chem. Phys.*, 2021, **222**, 2000311.
22 N. Corrigan, J. Yeow, P. Judzewitsch, J. Xu and C. Boyer, Seeing the Light: Advancing Materials Chemistry through Photopolymerization, *Angew. Chem., Int. Ed.*, 2019, **58**, 5170–5189.
23 M. Hartlieb, Photo-Iniferter RAFT Polymerization, *Macromol. Rapid Commun.*, 2022, **43**, 2100514.
24 L. Lu, H. Zhang, N. Yang and Y. Cai, Toward Rapid and Well-Controlled Ambient Temperature RAFT Polymerization under UV–Vis Radiation: Effect of Radiation Wave Range, *Macromolecules*, 2006, **39**, 3770–3776.
25 H. Wang, Q. Li, J. Dai, F. Du, H. Zheng and R. Bai, Real-Time and in Situ Investigation of "Living"/Controlled Photopolymerization in the Presence of a Trithiocarbonate, *Macromolecules*, 2013, **46**, 2576–2582.
26 T. G. McKenzie, Q. Fu, E. H. H. Wong, D. E. Dunstan and G. G. Qiao, Visible Light Mediated Controlled Radical Polymerization in the Absence of Exogenous Radical Sources or Catalysts, *Macromolecules*, 2015, **48**, 3864–3872.
27 J. Luo, M. Li, M. Xin, W. Sun and W. Xiao, Visible Light Induced RAFT Polymerization of 2-Vinylpyridine without Exogenous Initiators or Photocatalysts, *Macromol. Chem. Phys.*, 2016, **217**, 1777–1784.
28 J. Xu, S. Shanmugam, N. A. Corrigan and C. Boyer, in *Controlled Radical Polymerization: Mechanisms*, ed. K. Matyjaszewski, B. S. Sumerlin, N. V. Tsarevsky and J. Chiefari, American Chemical Society, Washington, DC, 2015, pp. 247–267.
29 C. Ding, C. Fan, G. Jiang, X. Pan, Z. Zhang, J. Zhu and X. Zhu, Photocatalyst-Free and Blue Light-Induced RAFT Polymerization of Vinyl Acetate at Ambient Temperature, *Macromol. Rapid Commun.*, 2015, **36**, 2181–2185.
30 J. G. Kennemur, Poly(vinylpyridine) Segments in Block Copolymers: Synthesis, Self-Assembly, and Versatility, *Macromolecules*, 2019, **52**, 1354–1370.
31 K. Nieswandt, P. Georgopanos, C. Abetz, V. Filiz and V. Abetz, Synthesis of Poly(3-vinylpyridine)-Block-Polystyrene Diblock Copolymers via Surfactant-Free RAFT Emulsion Polymerization, *Materials*, 2019, **12**, 3145.
32 K. Nieswandt, P. Georgopanos and V. Abetz, Well-defined polyvinylpyridine- block -polystyrene diblock copolymers via RAFT aqueous-alcoholic dispersion polymerization: synthesis and isoporous thin film morphology, *Polym. Chem.*, 2021, **12**, 2210–2221.
33 J. Xu and V. Abetz, Nonionic UCST-LCST Diblock Copolymers with Tunable Thermoresponsiveness Synthesized via PhotoRAFT Polymerization, *Macromol. Rapid Commun.*, 2021, **42**, 2000648.
34 J. Xu and V. Abetz, Double thermoresponsive graft copolymers with different chain ends: feasible precursors for covalently crosslinked hydrogels, *Soft Matter*, 2022, **18**, 2082–2091.
35 J. Xu and V. Abetz, Synthesis of a Degradable Hydrogel Based on a Graft Copolymer with Unexpected Thermoresponsiveness, *Macromol. Chem. Phys.*, 2022, **223**, 2200058.
36 M. Rubens, P. Latsrisaeng and T. Junkers, Visible light-induced iniferter polymerization of methacrylates enhanced by continuous flow, *Polym. Chem.*, 2017, **8**, 6496–6505.
37 J. Peng, Q. Xu, Y. Ni, L. Zhang, Z. Cheng and X. Zhu, Visible light controlled aqueous RAFT continuous flow polymerization with oxygen tolerance, *Polym. Chem.*, 2019, **10**, 2064–2072.
38 J. T. Lai, D. Filla and R. Shea, Functional Polymers from Novel Carboxyl-Terminated Trithiocarbonates as Highly

Efficient RAFT Agents, *Macromolecules*, 2002, **35**, 6754–6756.

39 H. Zhang, J. Deng, L. Lu and Y. Cai, Ambient-Temperature RAFT Polymerization of Styrene and Its Functional Derivatives under Mild Long-Wave UV–vis Radiation, *Macromolecules*, 2007, **40**, 9252–9261.

40 S. D. Sütekin and O. Güven, Preparation of poly(tert –butyl acrylate)–poly(acrylic acid) amphiphilic copolymers via radiation–induced reversible addition–fragmentation chain transfer mediated polymerization of tert –butyl acrylate, *Polym. Int.*, 2020, **69**, 693–701.

41 R. R. Gibson, A. Fernyhough, O. M. Musa and S. P. Armes, RAFT dispersion polymerization of N N -dimethylacrylamide in a series of n -alkanes using a thermoresponsive poly(tert -octyl acrylamide) steric stabilizer, *Polym. Chem.*, 2021, **12**, 2165–2174.

42 C. Capello, U. Fischer and K. Hungerbühler, What is a green solvent? A comprehensive framework for the environmental assessment of solvents, *Green Chem.*, 2007, **9**, 927.

43 D. Prat, J. Hayler and A. Wells, A survey of solvent selection guides, *Green Chem.*, 2014, **16**, 4546–4551.

44 Y. Zhou, K. Jiang, Q. Song and S. Liu, Thermo-induced formation of unimolecular and multimolecular micelles from novel double hydrophilic multiblock copolymers of N,N-dimethylacrylamide and N-isopropylacrylamide, *Langmuir*, 2007, **23**, 13076–13084.

45 J. Rieger, W. Zhang, F. Stoffelbach and B. Charleux, Surfactant-Free RAFT Emulsion Polymerization Using Poly(N,N -dimethylacrylamide) Trithiocarbonate Macromolecular Chain Transfer Agents, *Macromolecules*, 2010, **43**, 6302–6310.

46 C. Gao, Q. Li, Y. Cui, F. Huo, S. Li, Y. Su and W. Zhang, Thermoresponsive diblock copolymer micellar macro-RAFT agent-mediated dispersion RAFT polymerization and synthesis of temperature-sensitive ABC triblock copolymer nanoparticles, *J. Polym. Sci., Part A: Polym. Chem.*, 2014, **52**, 2155–2165.

47 H. Kang, Y. Su, X. He, S. Zhang, J. Li and W. Zhang, In situ synthesis of ABA triblock copolymer nanoparticles by seeded RAFT polymerization: Effect of the chain length of the third a block on the triblock copolymer morphology, *J. Polym. Sci., Part A: Polym. Chem.*, 2015, **53**, 1777–1784.

48 X. He, Y. Qu, C. Gao and W. Zhang, Synthesis of multicompartment nanoparticles of a triblock terpolymer by seeded RAFT polymerization, *Polym. Chem.*, 2015, **6**, 6386–6393.

49 K. H. Wong, T. P. Davis, C. Barner-Kowollik and M. H. Stenzel, Honeycomb structured porous films from amphiphilic block copolymers prepared via RAFT polymerization, *Polymer*, 2007, **48**, 4950–4965.

50 L. Sambe, K. Belal, F. Stoffelbach, J. Lyskawa, F. Delattre, M. Bria, F. X. Sauvage, M. Sliwa, V. Humblot, B. Charleux, G. Cooke and P. Woisel, Multi-stimuli responsive supramolecular diblock copolymers, *Polym. Chem.*, 2014, **5**, 1031–1036.

51 Y. Yang, J. Zheng, S. Man, X. Sun and Z. An, Synthesis of poly(ionic liquid)-based nano-objects with morphological transitions via RAFT polymerization-induced self-assembly in ethanol, *Polym. Chem.*, 2018, **9**, 824–827.

52 P. N. Kurek, A. J. Kloster, K. A. Weaver, R. Manahan, M. L. Allegrezza, N. de Alwis Watuthanthrige, C. Boyer, J. A. Reeves and D. Konkolewicz, How Do Reaction and Reactor Conditions Affect Photo-induced Electron/Energy Transfer Reversible Addition–Fragmentation Transfer Polymerization?, *Ind. Eng. Chem. Res.*, 2018, **57**, 4203–4213.

53 H. Tao, L. Xia, G. Chen, T. Zeng, X. Nie, Z. Zhang and Y. You, PET-RAFT Polymerization Catalyzed by Small Organic Molecule under Green Light Irradiation, *Polymers*, 2019, **11**, 892.

54 P. Vana, T. P. Davis and C. Barner-Kowollik, Kinetic Analysis of Reversible Addition Fragmentation Chain Transfer (RAFT) Polymerizations: Conditions for Inhibition, Retardation, and Optimum Living Polymerization, *Macromol. Theory Simul.*, 2002, **11**, 823–835.